17th AIAA/CEAS Aeroacoustics Conference (32nd AIAA Aeroacoustics Conference)
05 - 08 June 2011, Portland, Oregon

AIAA 2011-2837

A computational study of the effects of nozzle-exit turbulence level on the flow and acoustic fields of a subsonic jet

Christophe Bogey[*], **Olivier Marsden**[†] and **Christophe Bailly**[‡]

Laboratoire de Mécanique des Fluides et d'Acoustique

UMR CNRS 5509, Ecole Centrale de Lyon

69134 Ecully, France

Five isothermal round jets at Mach number M = 0.9 and diameter-based Reynolds number $\mathbf{Re_D = 10^5}$ originating from a pipe nozzle are computed by Large-Eddy Simulations to investigate the effects of initial turbulence on flow development and noise generation. In the pipe, the boundary layers are tripped in order to impose, at the nozzle exit, laminar mean velocity profiles of momentum thickness equal to 1.8% of the jet radius, yielding Reynolds number $\mathbf{Re_\theta = 900}$, and peak turbulence intensities of 0, 3, 6, 9 and 12% of the jet velocity. As the nozzle-exit turbulence level increases, the shear-layer development is strongly modified. Vortex roll-ups and pairings and, more generally, coherent structures gradually disappear, leading to lower shear-layer spreading rate and rms fluctuating velocities. The jets also develop farther downstream, resulting in longer potential cores. With rising exit turbulence intensity, the noise levels generated by the present jets at $\mathbf{Re_D = 10^5}$ are moreover found to decrease, and to tend asymptotically towards the levels measured for jets at Reynolds numbers higher than $\mathbf{5 \times 10^5}$, which are likely to be initially turbulent and to emit negligible vortex-pairing noise. These results correspond well to experimental observations available in the literature, usually obtained separately for either mixing layers, jet flow or sound fields.

I. Introduction

Since the seminal work done by Crow and Champagne[1] and Brown and Roshko[2] on coherent structures, the effects of the initial conditions in mixing layers and jets have been investigated in a large number of experiments over the past forty years. As reported in the review papers written by Crighton,[3] Hussain,[4] Gutmark and Ho,[5] and Ho and Huerre,[6] these effects have been found to be strong, and hence recognized as one of the reasons of the discrepancies observed between data of the literature for such flows. The initial conditions of a free shear layer have also been shown to be characterized by three main parameters, namely the Reynolds number Re_θ based on the shear-layer momentum thickness δ_θ, the (laminar, transitional or turbulent) flow state, and the peak fluctuation intensity with respect to the jet velocity u'_e/u_j. On this matter, the reader can refer for instance to the two thorough publications by Hussain and Zedan.[7,8]

The last two parameters mentioned above, *i.e.* the initial flow state and disturbance levels, are inherently linked. Indeed, in broad outline, the initial states of a shear layer can be divided into two main categories: laminar (or weakly disturbed) states when the peak fluctuation intensity u'_e/u_j is not appreciably higher than 1%, and turbulent (or highly disturbed) states when u'_e/u_j is around 10%. The transition from laminar to turbulent flow takes place in the mixing layer in the first case, but moves to the nozzle boundary layers in the second case, which is very likely to cause significant changes in the turbulent and acoustic features of free shear flows as pointed out by Mollo-Christensen *et al.*[9] These changes have been studied in several experiments, in particular by tripping the boundary layers, thus generating exit turbulent conditions, for

[*]CNRS Research Scientist, AIAA Member, christophe.bogey@ec-lyon.fr

[†]Assistant Professor at Ecole Centrale de Lyon, AIAA Member, olivier.marsden@ec-lyon.fr

[‡]Professor at Ecole Centrale de Lyon & Institut Universitaire de France, Senior AIAA Member, christophe.bailly@ec-lyon.fr

jets at moderate diameter-based Reynolds numbers around $\mathrm{Re}_D = 10^5$ whose initial state would otherwise be laminar.

The impact of initial disturbances on the development of mixing layers has first be considered, as is the case for example in the works of Batt,[10] Hussain and Zedan,[7,8] Husain and Hussain,[11] Hussain and Husain,[12] and Bell and Mehta.[13] Mixing layers with laminar upstream conditions have been shown to grow at a higher rate with an overshoot in turbulence intensity around the first stage of vortex merging. The formation and perseverance of coherent eddies in shear layers in the presence of free stream turbulence have also been discussed by Chandrsuda *et al.*[14] and Wygnanski *et al.*[15] Similarly, the effects of laminar/turbulent initial conditions have been examined for jets. Jets with exit laminar boundary layers have been found to develop more rapidly in the experiments of Hill *et al.*,[16] Russ and Strykowski[17] and Xu and Antonia,[18] among others. The influence of inlet velocity fluctuations on the control of jets subjected to tonal excitation has also been explored by Zaman and Hussain,[19] Zaman,[20] Lepicovsky and Brown,[21] and Raman *et al.*[22,23] Finally, as stated in papers by Lilley[24] and Harper-Bourne,[25] noise generation in subsonic jets appears to depend strongly on the initial flow state. Additional noise components, attributed to shear-layer vortex pairings, have been obtained for initially laminar jets by Maestrello and McDaid,[26] Grosche,[27] Zaman,[28] and Bridges and Hussain.[29]

The experiments listed above demonstrated the importance of laminar/turbulent initial conditions in free shear flows. In most cases, however, the effects of the turbulence level cannot be clearly distinguished from those of other parameters, such as the shape or the thickness of the boundary layers, which may also vary. Some careful investigations have fortunately been performed, such as those by Hussain and Zedan[7,8] dealing with variations in the momentum-thickness Reynolds number Re_θ at fixed u'_e/u_j and, conversely, in u'_e/u_j at fixed Re_θ for both laminar and turbulent initial shear layers. In the latter case, laminar velocity profiles at $\mathrm{Re}_\theta = 200$ with u'_e/u_j between 8.4% and 17.2% were in particular considered.

The present work, in the same way, aims to study the influence of the initial turbulence on subsonic jets characterized by identical laminar mean velocity profiles but peak turbulence intensities u'_e/u_j ranging from 0 to 12% at the nozzle exit. It has been made possible thanks to the increase in computer power, and to the rapid progress in the field of computational aeroacoustics since the three-dimensional jet simulations of Freund[30] and Bogey *et al.*,[31] see the reviews by Colonius and Lele,[32] Bogey and Bailly[33] and Wang *et al.*[34] for instance. Indeed, simulations can now be used as numerical experiments under controlled conditions to improve our knowledge on jet flows, as illustrated in Bogey *et al.*[35,36]

This work is a natural continuation of our previous Large-Eddy Simulations (LESs) of subsonic jets. Following a preliminary attempt to compute an initially turbulent jet in Bogey *et al.*,[37] two studies have recently been carried out for jets at Mach number $\mathrm{M} = 0.9$ and Reynolds numbers $\mathrm{Re}_D = 10^5$. In the first study, detailed in Bogey and Bailly,[38] the jets are initially laminar, leading to strong vortex pairings in the shear layers. In the second one, in Bogey *et al.*,[39,40] the jets are made initially nominally turbulent by tripping the boundary layers inside a pipe nozzle. At the exit, Blasius velocity profiles of momentum thickness $\delta_\theta/r_0 = 1.8\%$ and peak axial turbulent intensities $u'_e/u_j = 9\%$ are specified (r_0 is the pipe radius), in agreement with the initial conditions measured in tripped jets by Zaman.[20,28] The final LES using a grid of 252 million points are shown to provide shear-layer solutions that are practically grid-converged and, more generally, results that can be regarded as numerically accurate as well as physically relevant. The jet mixing layers, while exhibiting a wide range of turbulent scales, are also found to display attenuated but persistent vortex pairings.

In the present paper, LESs of five round isothermal jets at Mach number $\mathrm{M} = 0.9$ and Reynolds number $\mathrm{Re}_D = 10^5$, performed at high resolution using grids of 252 million points, low-dissipation schemes and relaxation filtering as a subgrid dissipation model, are reported. For all jets, laminar mean velocity profiles of momentum thickness $\delta_\theta/r_0 = 1.8\%$, yielding a Reynolds number $\mathrm{Re}_\theta = 900$, are imposed inside a pipe nozzle. As for the exit peak turbulence intensities u'_e/u_j, their values are respectively fixed to 0, 3, 6, 9 and 12% by tripping the boundary layers in the pipe. The influence of the initial turbulence level on the mean and turbulent flow fields as well as on the acoustic far field is systematically investigated. Particular attention is paid to the changes in the shear-layer transition as nozzle-exit disturbances gradually increase, and to their consequences on noise generation mechanisms including pairings of coherent structures. Comparisons are also made with measurements available in the literature for jets at Reynolds numbers $\mathrm{Re}_D \geq 5 \times 10^5$, in order to examine the possible convergence of the results obtained for the present jets at $\mathrm{Re}_D = 10^5$ towards typical high Reynolds number data as the exit turbulence intensity rises.

The paper is organized as follows. In section II, the parameters of the jet LESs and of the extrapolation

of the LES near field to the far field, including numerical algorithm, computational grids and times, are presented. In section III, the initial conditions in the different jets are first characterized. The shear-layer and jet flow fields as well as the acoustic fields are then shown and analyzed. Concluding remarks are provided in section IV.

II. Simulation parameters

A. Jet definition

Five isothermal round jets at Mach number $M = u_j/c_a = 0.9$ and Reynolds number $Re_D = u_j D/\nu = 10^5$ are considered (u_j is the jet inflow velocity, c_a is the ambient speed of sound, D is the nozzle diameter, and ν is the kinematic molecular viscosity). They originate from a pipe nozzle of radius $r_0 = D/2$ and length $2r_0$ as represented in figure 1. The ambient temperature and pressure are $T_a = 293$ K and $p_a = 10^5$ Pa. At the nozzle-exit section at $z = 0$, the width of the nozzle lip is $0.053r_0$. At the pipe inlet at $z = -2r_0$, laminar Blasius boundary layers of thickness $\delta = 0.15r_0$, or equivalently of momentum thickness $\delta_\theta = 0.018r_0$ yielding a Reynolds number $Re_\theta = u_j\delta_\theta/\nu = 900$, are imposed. The axial velocity profile is given by a polynomial approximation of the Blasius profile. Radial and azimuthal velocities are initially set to zero, pressure is kept constant at its ambient value, and the temperature is determined by a Crocco-Busemann relation.

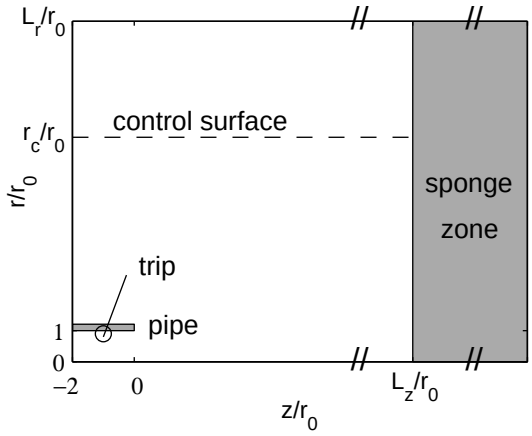

Figure 1. Visualization in the (z, r) plane of the simulation configuration (the pipe thickness is here multiplied by 4). See in table 1 for the values of r_c, L_r and L_z.

In four LESs referred to as Jet3%, Jet6%, Jet9%, and Jet12%, the jet boundary layers are tripped inside the pipe by adding random low-level vortical disturbances decorrelated in the azimuthal direction. The tripping is applied at $z = -r_0$ in the first three simulations and at $z = -0.2r_0$ in the fourth one. The tripping magnitudes are empirically chosen in order to obtain, at the pipe exit, peak turbulence intensities u'_e/u_j equal to 3, 6, 9 and 12% in Jet3%, Jet6%, Jet9%, and Jet12%, respectively, as well as mean-velocity profiles in agreement with the laminar profiles imposed at the pipe inlet, which will be illustrated in section III.A. As evidenced by the experiments of Hussain and Zedan[7,8] and Zaman[20,28] for instance, it is indeed possible to find high levels of velocity fluctuations together with laminar velocity profiles close to the nozzle exit of tripped jets. In a fifth LES referred to as Jet0%, no boundary-layer tripping is used in order to consider also an initially fully laminar jet. Note that Jet9% corresponds exactly to the simulation Jetring1024drdz in Bogey *et al.*,[39] where the tripping method is described in detail, and is shown to generate negligible spurious acoustic waves. In that reference, the very weak sensitivity of the LES results with respect to the tripping methodology is also displayed.

B. LES procedure and numerical methods

The numerical methodology is identical to that used for recent jet simulations in Bogey *et al.*[38–40] The LES are carried out using a solver of the three-dimensional filtered compressible Navier-Stokes equations in cylindrical coordinates (r, θ, z) using low-dissipation and low-dispersion finite differences developed in Bogey and Bailly.[41] The axis singularity is taken into account by the method of Mohseni and Colonius.[42]

Fourth-order eleven-point centered finite differences are used for spatial discretization, and a second-order six-stage low-storage Runge-Kutta algorithm is implemented for time integration. To circumvent the time-step restriction induced by the cylindrical coordinates, the derivatives in the azimuthal direction around the axis are calculated using every n-th grid point, from $n = 2$ up to $n = 64$ near the centerline, as described in Bogey *et al.*[43] To remove grid-to-grid oscillations, a sixth-order eleven-point centered filter designed to mainly damp the shortest waves discretized in Bogey *et al.*[44] is applied explicitly to the flow variables every time step. The discretization at the boundaries is performed by non-centered finite differences and filters with properties optimized in the Fourier space, provided in Bogey *et al.*[38] and Berland *et al.*[45]

The explicit filtering is also employed as a subgrid dissipation model to relax turbulent energy from scales at wave numbers close to the grid cut-off wave number while leaving larger scales mostly unaffected, as suggested by Visbal and Rizzetta.[46] This LES approach is developed to avoid difficulties in defining the effective flow Reynolds number, which might be the case when using eddy-viscosity models as pointed out by Domaradzki and Yee.[47] More details on the LES-RF approach based on relaxation filtering are available in Bogey and Bailly.[48–50] The accuracy of the LES fields from the present simulation Jet9% is investigated in Bogey *et al.*,[39] in which Jet9% is called Jetring1024drdz, based on the tranfer functions associated with molecular viscosity, relaxation filtering and time integration. In that LES, molecular viscosity is shown to be the dominant dissipation mechanism for the scales discretized at least by six or seven points per wavelength. The physics of the larger turbulent structures is therefore expected not to be governed by numerical or subgrid-modeling dissipation, and the effective flow Reynolds number should thus not be artificially decreased.

Finally, in order to compute the radiated noise directly, the non-reflective boundary conditions of Tam and Dong[51] are specified, with the addition of a sponge zone at the outflow. The non-reflective conditions are also applied at the pipe inlet.

C. Simulation parameters

The computational setup is illustrated in figure 1, and some numerical parameters are provided in table 1. The LESs are performed using two grids, one for Jet0%, another for Jet3%, Jet6%, Jet9%, and Jet12%, both containing $n_r \times n_\theta \times n_z = 256 \times 1024 \times 962 = 252$ million points. They are identical to the grids employed for the simulations referred to respectively as Jetring1024dz and Jetring1024drdz (that is also Jet9%) in Bogey *et al.*[39,40] In the grid used for Jet0%, the minimum mesh spacings in the radial, azimuthal and axial directions are $\Delta r/r_0 = 0.0072$, $r_0\Delta\theta/r_0 = 0.0061$ and $\Delta z/r_0 = 0.0072$, corresponding to $\Delta r/\delta_\theta(0) = 0.40$, $r_0\Delta\theta/\delta_\theta(0) = 0.34$ and $\Delta z/\delta_\theta(0) = 0.40$ when normalized by the nozzle-exit boundary-layer thickness $\delta_\theta(0)$. In the grid used for the tripped jets, the discretizations in the azimuthal and axial directions are the same as previously, but the radial resolution is twice as high along the lip line with $\Delta r/r_0 = 0.0036$ at $r = r_0$. The physical domains, excluding the eighty-point outflow sponge zones, extend axially up to $L_z = 25r_0$, and radially up to $L_r = 11r_0$ in Jet0% and $L_r = 9r_0$ in the other LESs.

Table 1. Simulation parameters: numbers of grid points n_r, n_θ, n_z, mesh spacings Δr at $r = r_0$, $r_0\Delta\theta$, and Δz at $z = 0$, extents L_r, L_z of the physical domain, radial position r_c of the control surface, and time duration T.

	n_r, n_θ, n_z	$\Delta r/r_0$	$r_0\Delta\theta/r_0$	$\Delta z/r_0$	L_r, L_z	r_c/r_0	Tu_j/r_0
Jet0%	$256, 1024, 962$	0.72%	0.61%	0.72%	$11r_0, 25r_0$	7.25	325
Jet3%, Jet6%, Jet9%, Jet12%	$256, 1024, 962$	0.36%	0.61%	0.72%	$9r_0, 25r_0$	6.5	375

The mesh spacings are uniform in the azimuthal direction, but vary in the axial and radial directions as represented in figure 2. In figure 2(a), the axial mesh size is minimum, and constant between $z = -r_0$ and $z = 0$, that is between the trip location in Jet3%, Jet6% and Jet9% and the pipe exit, with $\Delta z/r_0 = 0.0072$. Upstream of $z = -r_0$, the grid is stretched up to the inlet, leading to 169 points in the pipe. Downstream of the nozzle, a grid stretching is applied at rates lower than 1%, allowing to reach $\Delta z/r_0 = 0.065$ at $z = 13.3r_0$. In figure 2(b), the radial mesh sizes are minimum around $r = r_0$, with $\Delta r/r_0 = 0.0072$ in Jet0% and $\Delta r/r_0 = 0.0036$ in the other LESs as mentioned above. The grids are then stretched at rates lower than 4% to preserve numerical accuracy. The inlet boundary layers are thus discretized by 19 points in the untripped jet and 31 points in the tripped jets, for respectively 62 and 77 points within the pipe radius. The maximum radial mesh sizes are obtained for $r \geq 3r_0$, and are equal to $\Delta r/r_0 = 0.065$ in Jet0% and $\Delta r = 0.081r_0$ otherwise, yielding Strouhal numbers of $\mathrm{St}_D = fD/u_j = 8.6$ and 6.9 for acoustic waves

discretized by four points par wavelength (f is the time frequency).

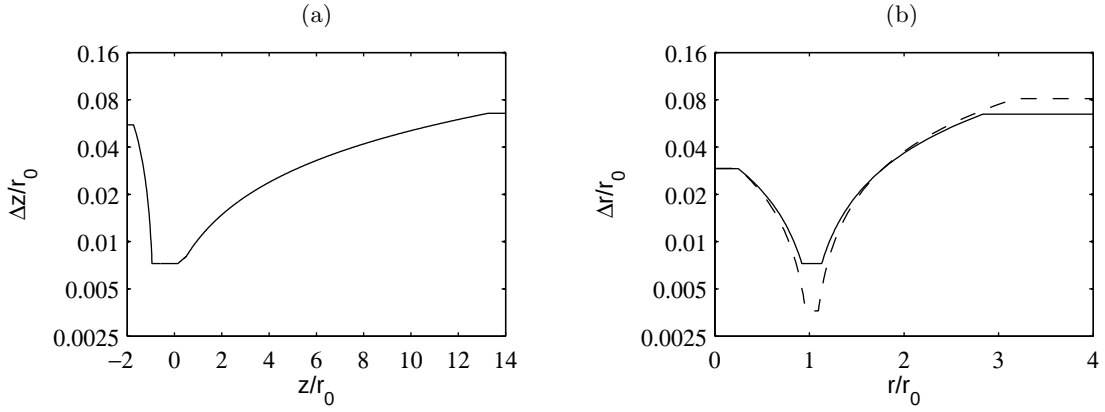

Figure 2. Representation, in logarithmic scales, of axial and radial mesh spacings (a) Δz for $-2 \leq z/r_0 \leq 14$ in all simulations, and (b) Δr for $0 \leq r/r_0 \leq 4$ in ——— Jet0%, − − − Jet3%, Jet6%, Jet9% and Jet12%.

The quality of the shear-layer discretization in the simulation Jet9% (also referred to as Jetring1024drdz in other papers) is assessed in Bogey *et al.*[39] In that reference, the ratios between the integral length scales of the axial fluctuating velocity and the local mesh sizes along the lip line are considered. They typically fall within a range of 4 to 10, suggesting that the grid resolution is appropriate in the three coordinate directions. An additional simulation is also carried out using the same grid for an axisymmetric mixing layer in which all nozzle-exit conditions are identical except for the boundary-layer thickness which is doubled. The properties of the initial turbulence and of the shear-layer flow fields obtained from Jet9% and the latter simulation are in good agreement, showing that they are practically grid-converged. The solutions from Jet9%, as well as from Jet3%, Jet6%, and Jet12% using the same mesh grid, are consequently expected to be accurate. Despite a lower radial resolution, leading to a total of 19 points within the inlet boundary layers instead of 31, the remark above most probably also applies to the results from Jet0% because of the initially fully laminar state of the jet in that case. This assertion is supported by LESs of the same kind reported in Bogey and Bailly,[38] providing very similar results for an initially fully laminar jet using 7 or 14 points within the upstream boundary layers.

The simulation times, given in table 1, are equal to $325r_0/u_j$ in Jet0% and $375r_0/u_j$ in the other LESs. Density, velocity components and pressure are recorded from time $t = 125r_0/u_j$ at every point along the jet axis, and on the two surfaces at $r = r_0$ and $r = r_c = 7.25r_0$ in Jet0% ($t = 100r_0/u_j$ and $r_c = 6.5r_0$ otherwise), at a sampling frequency allowing the computation of spectra up to a Strouhal number of 20. The velocity spectra are evaluated from overlapping samples of duration $27.4r_0/u_j$. The flow statistics are determined from $t = 175r_0/u_j$, and they are averaged in the azimuthal direction.

The simulations have been performed using NEC SX-8 computers, on 7 processors using OpenMP, leading to a CPU speed of around 36 Gflops. Each of the four LES of tripped jets Jet3%, Jet6%, Jet9% and Jet12% required in particular around 7,000 CPU hours and 60 Gb of memory for 164,000 time steps.

D. Far-field extrapolation

The LES near fields are propagated to the acoustic far field by solving the isentropic linearized Euler equations (ILEE) in cylindrical coordinates. The extrapolation is performed from fluctuating velocities and pressure recorded in the LESs on a surface at $r = r_c$ as reported in the previous section, see also in figure 1. These data are interpolated onto a cylindrical surface discretized by an axial mesh spacing of $\Delta z = 0.065r_0$. They are then imposed at the bottom boundary of the grid on which the ILEE are solved using the same numerical schemes and boundary conditions as in the LESs. This grid contains $n_r \times n_\theta \times n_z = 835 \times 256 \times 1155$ points for Jet0%, and $845 \times 256 \times 1155$ points for Jet3%, Jet6%, Jet9% and Jet12%, and extends axially from $z = -16.6r_0$ to $58.2r_0$ and radially up to $r = 61.4r_0$. The grid spacings are uniform with $\Delta r = \Delta z = 0.065r_0$, yielding a Strouhal number of $\mathrm{St}_D = 8.6$ for four points per wavelength. After a propagation time of $t = 60r_0/u_j$, pressure is recorded around the jets at a distance of $60r_0$ from $z = r = 0$, where far-field acoustic conditions are expected to apply according to the experiments of Ahuja *et al.*,[52] during periods of $175r_0/u_j$ for Jet0%, and $250r_0/u_j$ for the other jets. Pressure spectra are evaluated using overlapping samples of duration $38r_0/u_j$, and they are averaged in the azimuthal direction.

III. Results

A. Initial flow conditions

The profiles of mean and rms axial velocities obtained at the pipe exit for the five simulated jets are presented in figure 3. The mean velocity profiles, in figure 3(a), are all similar to the Blasius profiles specified at the pipe inlet, leading to the exit boundary-layer momentum thicknesses and shape factors collected in table 2, varying only from $\delta_\theta(0) = 0.0175r_0$ and $H = 2.55$ in Jet0% to $\delta_\theta(0) = 0.0188r_0$ and $H = 2.33$ in Jet12%. In figure 3(b), the peak intensities of velocity fluctuations in the different jets are noted to be close to 0, 3, 6, 9 and 12% respectively, as intended, see in table 2 for the exact values. The states of the nozzle-exit boundary layers in the present jets thus fall into the three following categories: fully laminar for Jet0%, nominally laminar for Jet3%, and nominally turbulent for Jet6%, Jet9% and Jet12%, according to the words of Zaman.[20,28] The initial conditions in Jet9% are also shown to be comparable to those measured in a tripped jet at $\mathrm{Re}_D = 10^5$ by the author mentioned above.

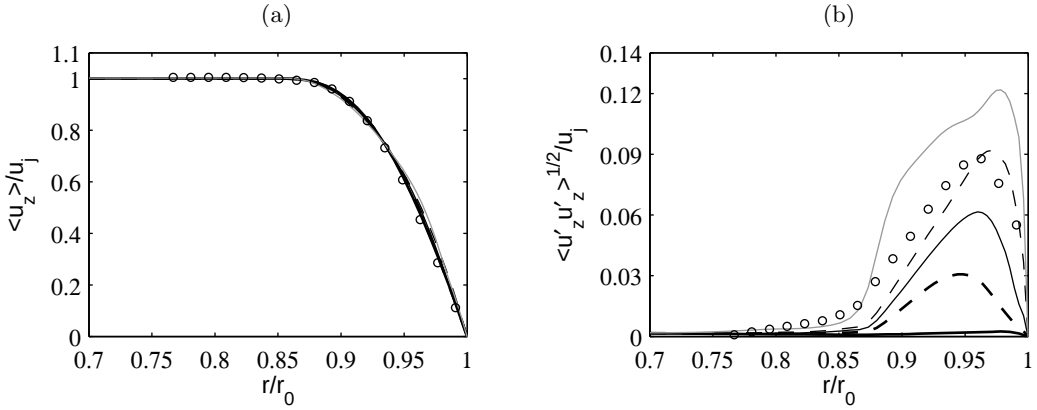

Figure 3. Profiles at $z = 0$ (a) of mean axial velocity $< u_z >$, and (b) of the rms values of fluctuating axial velocity u'_z: ——— Jet0%, – – – Jet3%, ——— Jet6%, – – – Jet9%, ——— Jet12%; ∘ measurements of Zaman[20,28] for a Mach 0.18, tripped jet at $\mathrm{Re}_D = 10^5$.

As an important characteristic of the initial jet flow, the integral length scales $L^{(\theta)}_{uu}$ estimated from the axial fluctuating velocity u'_z in the azimuthal direction at $r = r_0$ and $z = 0.4r_0$ are given in table 2. It is found that $L^{(\theta)}_{uu} = 2.1r_0$ in Jet0% and $L^{(\theta)}_{uu} = 0.14r_0$ in Jet3%, and that $L^{(\theta)}_{uu} < 0.02r_0$ in Jet6%, Jet9% and Jet12%. The azimuthal correlation of velocity disturbances just downstream of the pipe lip is consequently high in the untripped, initially fully laminar jet, but strongly decreases in the tripped jets with the exit turbulence level as previously observed in Bogey and Bailly.[38] In the three initially nominally turbulent jets, notably, the azimuthal velocity correlations are quite low, and the integral length scales $L^{(\theta)}_{uu}$ are roughly equal to or slightly smaller than the shear-layer momentum thickness $\delta_\theta(0)$.

Table 2. Initial jet parameters: boundary-layer momentum thickness $\delta_\theta(0)$, shape factor H, and peak turbulence intensities u'_e at the nozzle exit, and integral length scale $L^{(\theta)}_{uu}$ of velocity u'_z in the azimuthal direction at $r = r_0$ and $z = 0.4r_0$.

	$\delta_\theta(0)/r_0$	H	u'_e/u_j	$L^{(\theta)}_{uu}/r_0$
Jet0%	0.0175	2.55	0.25%	2.059
Jet3%	0.0176	2.52	3.07%	0.144
Jet6%	0.0179	2.48	6.15%	0.019
Jet9%	0.0185	2.36	9.18%	0.013
Jet12%	0.0188	2.33	12.19%	0.010

The properties of the jet initial disturbances are examined in more detail by calculating spectra of the fluctuating axial velocity at $r = r_0$ and $z = 0.4r_0$ near the nozzle lip. The spectra thus determined are represented as a function of the Strouhal number $\mathrm{St}_D = fD/u_j$ in figure 4(a), and of the dimensionless azimuthal wave number k_θ in figure 4(b). The spectra obtained in Jet0% show typical features of an initially fully laminar jet. The initial turbulence, albeit at a low level, is indeed dominated in that case

by highly distinctive frequency and azimuthal components. In particular, the contributions of the two first modes $k_\theta = 0$ and $k_\theta = 1$ are very high, whereas those from higher modes $k_\theta > 2$ are negligible.

On the contrary, the spectra obtained for the tripped jets in Jet3%, Jet6%, Jet9% and Jet12% all display broadband shapes, which are seen not to change much with the initial fluctuation level. For the four jets, the frequency spectra in figure 4(a) are rather flat up to $\mathrm{St}_D \simeq 1$ and rapidly decrease for higher Strouhal numbers, while the spectra in figure 4(b) show a distribution of turbulent energy over a wide range of azimuthal modes. In the latter spectra, significant components moreover clearly emerge around $k_\theta \simeq 44$. These components are weaker than the first low-order modes $k_\theta = 0, 1, 2$ in Jet3% for the initially nominally laminar jet. However, as their relative contributions increase with the nozzle-exit turbulence intensity, they are dominating in Jet9% and Jet12% for the two jets with highest initial disturbance levels.

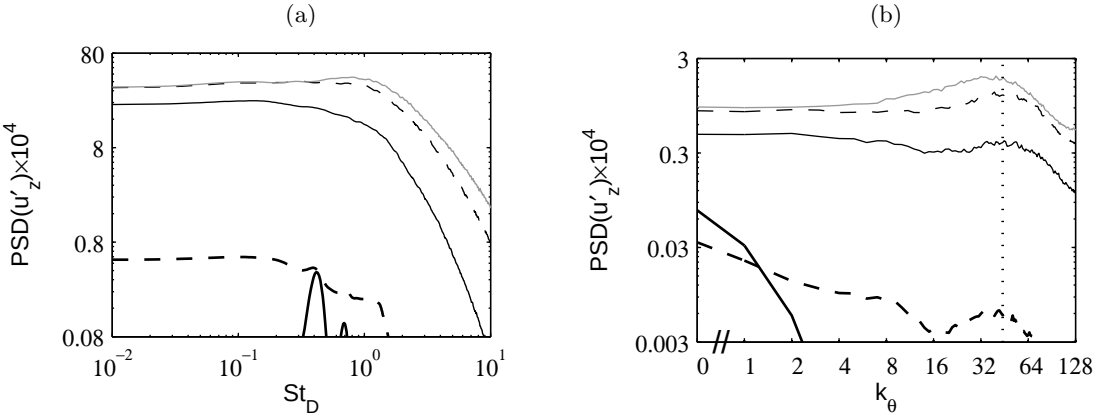

Figure 4. Power spectral densities (PSD) normalized by u_j of fluctuating velocity u'_z at $r = r_0$ and $z = 0.4r_0$, as functions (a) of Strouhal number $\mathrm{St}_D = fD/u_j$ and (b) of azimuthal wavenumber k_θ: ——— Jet0%, – – – Jet3%, ——— Jet6%, – – – Jet9%, ——— Jet12%. The dotted line indicates $k_\theta = 44$.

The physical relevance of the initial velocity spectra in Jet9% is discussed in Bogey *et al.*,[40] in which the spectra are re-plotted versus axial and azimuthal wave numbers $k_z\delta$ and $k_\theta\delta/r_0$, using a scaling with the boundary-layer thickness δ frequently encountered in the literature for wall-bounded flows. A very good qualitative agreement is obtained with spectra obtained by Eggels *et al.*[53] in a fully turbulent pipe flow using Direct Numerical Simulation. The wave numbers dominating in the azimuthal direction around $k_\theta\delta/r_0 \simeq 7$ are also found to be consistent with measurements of spanwise energy distribution in turbulent boundary layers provided by Tomkins and Adrian.[54] It seems therefore that the initial turbulent structures in the present tripped jets are organized in a similar fashion to those in turbulent wall-bounded flows, and that the remarkable azimuthal components noticed around $k_\theta \simeq 44$ in figure 4(b) are related to the basic physics of such flows.

B. Shear-layer development

Snapshots of the vorticity norm obtained in the five different jets just downstream of the pipe lip between $z = 0$ and $z = 3.75r_0$ are presented in figure 5. For low initial velocity fluctuations in Jet0% and Jet3%, the shear layers are (fully or nominally) laminar at $z = 0$, leading to laminar-turbulent flow transitions dominated by roll-ups and pairings of large vortical structures. With increasing nozzle-exit disturbance level, the shear layers tend towards being initially turbulent, which naturally makes vortex roll-up disappear. More interestingly, the development of the mixing layers gradually displays enhanced fine-scale turbulence as well as weaker large-scale structures. This is especially the case in figure 5(e) for the jet with peak turbulence intensity $u'_e/u_j \simeq 12\%$, for which it is quite difficult to distinguish coherent structures or pairing processes in the shear layers.

In order to shed light on the generation of 3-D motions in the jet mixing layers, snapshots of the axial vorticity ω_z obtained in three sections located at $z = r_0$, $z = 2r_0$ and $z = 4r_0$ are presented in figure 6. In Jet0%, in figure 6(a), the axial vorticity field is of negligible amplitude at $z = 0$, shows a small number of spots of significant level at $z = 2r_0$, and then is developed at $z = 4r_0$. This indicates that the flow in the initially fully laminar jet is nearly axisymmetric at the first position, starts its transition towards three-dimensionality around the second one, and is turbulent at the third one, in agreement with the vorticity

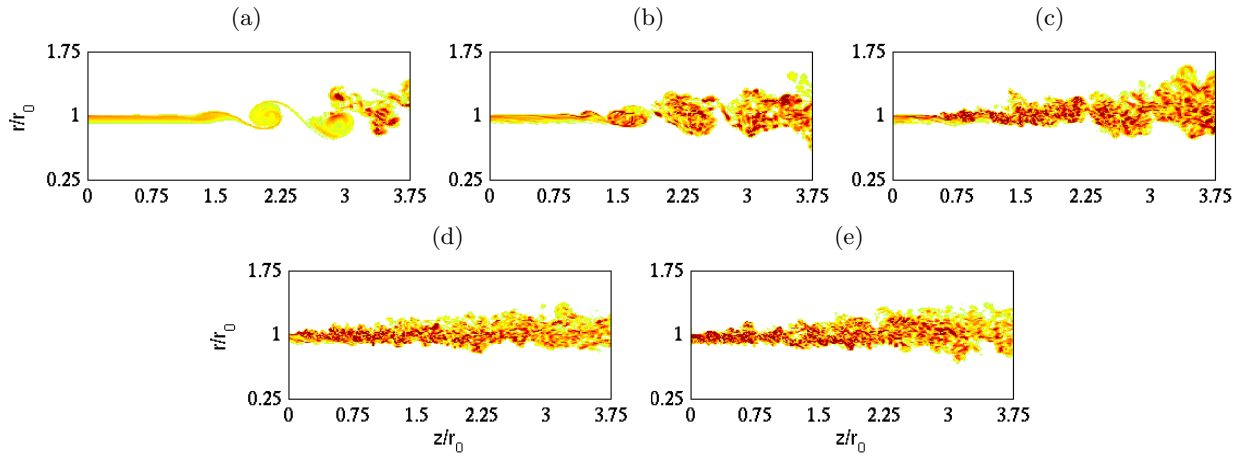

Figure 5. Snapshots in the (z, r) plane of vorticity norm $|\omega|$ in the shear layer just downstream of the pipe lip: (a) Jet0%, (b) Jet3%, (c) Jet6%, (d) Jet9%, (e) Jet12%. The colour scale ranges up to the level of $25u_j/r_0$.

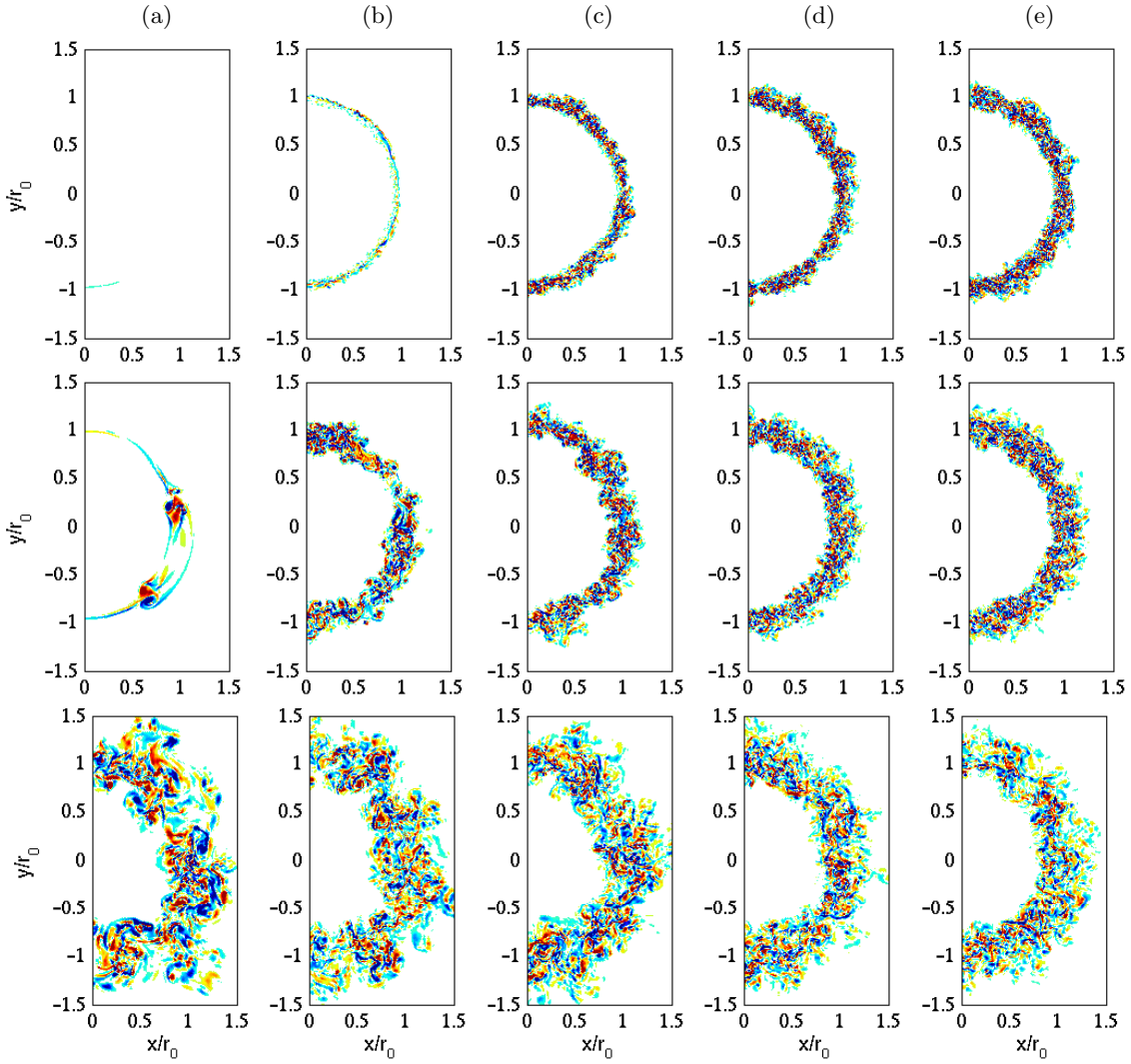

Figure 6. Snapshots in the (r, θ) or (x, y) planes at $z = r_0$, $2r_0$ and $4r_0$, from top to bottom, of axial vorticity ω_z: (a) Jet0%, (b) Jet3%, (c) Jet6%, (d) Jet9%, (e) Jet12%. The colour scale ranges from levels from -13 to $13u_j/r_0$. Only $x \geq 0$ is shown.

snapshot of figure 5(a). In Jet3%, 3-D structures are already clearly visible at $z = 2r_0$ in figure 6(b), implying that the laminar-turbulent flow transition occurs farther upstream in that case, as it can also be inferred from figure 5(b). In the three other LESs dealing with initially nominally turbulent jets, unsurprisingly, 3-D turbulent fields are observed in figures 6(c), 6(d) and 6(e) in the three planes considered. These fields may however contain more fine scales for higher initial turbulence levels, see the vorticity snapshots from Jet6% and Jet12% at $z = 4r_0$ for instance.

To obtain rough approximations of the sizes of the turbulent structures in the mixing layers, the axial and azimuthal integral length scales $L_{uu}^{(z)}$ and $L_{uu}^{(\theta)}$ are evaluated from the fluctuating velocity u'_z at $r = r_0$ along the lip line. Their variations between $z = 0$ and $z = 10r_0$ are presented in figure 7. In figure 7(a), after a transitional period corresponding very probably to the flow adjustment following the nozzle lip from a boundary-layer profile to a shear-layer profile, the axial length scales $L_{uu}^{(z)}$ are observed to grow fairly linearly, as typically found experimentally from the work by Davies *et al.*[55] to the measurements of Fleury *et al.*[56] More importantly, these scales are seen to become gradually smaller as the initial turbulence intensity increases in the jets. Similar trends are noted for the azimuthal length scales $L_{uu}^{(\theta)}$ in figure 7(b). The influence of the exit disturbance level appears however stronger on the azimuthal than on the axial length scales, especially during the early stage of mixing-layer development. Downstream of the nozzle lip, the azimuthal length scales, whose values at $r = r_0$ and $z = 0.4r_0$ are given in table 2, are indeed much larger in Jet0% and Jet3% for the two initially laminar jets than in the other LESs.

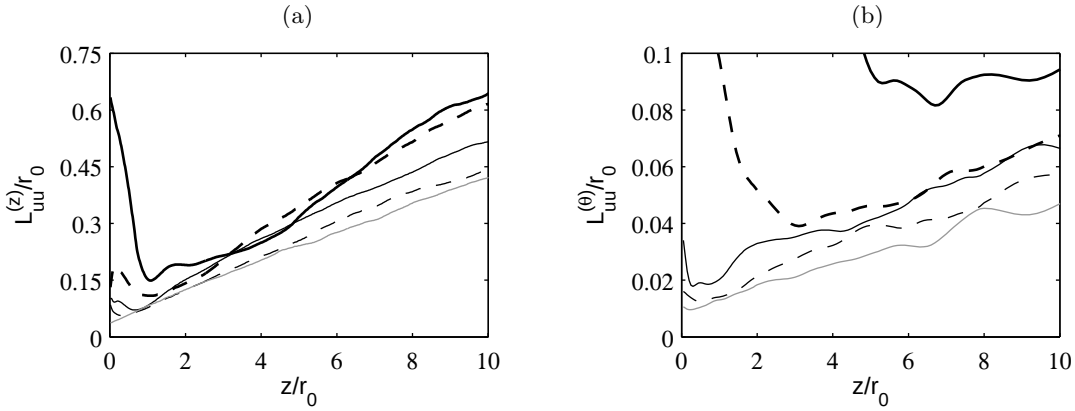

Figure 7. Variations of axial and azimuthal integral length scales (a) $L_{uu}^{(z)}$ and (b) $L_{uu}^{(\theta)}$ calculated from velocity u'_z at $r = r_0$: ——— Jet0%, – – – Jet3%, ——— Jet6%, – – – Jet9%, ——— Jet12%.

The variations over $0 \leq z \leq 10r_0$ of the shear-layer momentum thickness δ_θ are presented in figure 8(a) for the different jets. With increasing nozzle-exit turbulence level, the mixing-layer growth begins closer to the exit section, at a position ranging from $z \simeq 1.5r_0$ in Jet0% to $z \simeq 0$ in Jet9% and Jet12%, as expected from the vorticity fields of figure 5. It then occurs at a much lower rate resulting in a slower overall flow development. To illustrate this point quantitatively, the variations of the spreading rate $\mathrm{d}\delta_\theta/\mathrm{d}z$ are shown in figure 8(b). Higher initial disturbances in the jets clearly lead to lower spreading rates. The decrease is particularly significant for their peak values, wich are equal to 0.057 in Jet0%, 0.045 in Jet3%, 0.033 in Jet6% and 0.024 in Jet9%. Similar behaviour has been found experimentally for mixing layers by Hussain and Zedan,[8] Husain and Hussain,[11] and Bell and Mehta.[13] Husain and Hussain[11] notably considered axisymmetric mixing layers with laminar or turbulent upstream conditions, characterized by Reynolds numbers $\mathrm{Re}_\theta \simeq 400$ and initial turbulence intensities $u'_e/u_j \simeq 3\%$ in the former case, and by $\mathrm{Re}_\theta \simeq 1400$ and $u'_e/u_j \simeq 10\%$ in the latter. They obtained maximum spreading rates between 0.06 and 0.08 for laminar conditions but around 0.03 for turbulent conditions, which agrees well with the present LES results.

The peak rms values of axial, radial and azimuthal velocities u'_z, u'_r and u'_θ and the maximum Reynolds shear stresses $< u'_r u'_z >$ evaluated between $z = 0$ and $z = 10r_0$ are represented in figure 9. In Jet0%, maximum intensities around 22% are achieved for all velocity components. The profiles also exhibit dual-peak shapes, which is typical of a first stage of strong vortex pairings in the mixing layers according to experimental and numerical data from Zaman and Hussain[19] and Bogey and Bailly,[38] among others. As u'_e/u_j increases at the nozzle exit, the turbulence intensities start to rise farther upstream in the shear layers, but lower peak values are reached. The reduction in rms velocity values and Reynolds shear stresses when specifying higher initial disturbances is significant, as shown in table 3. This is especially the case for the radial velocity u'_r,

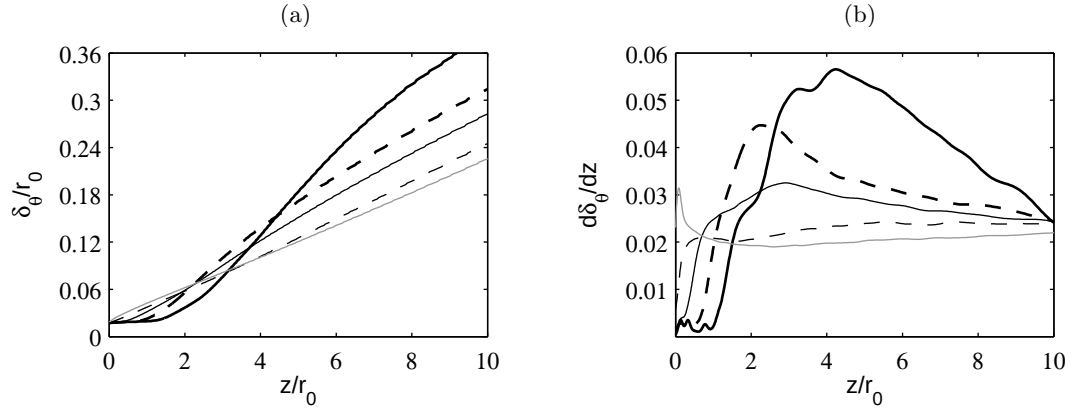

Figure 8. Axial variations (a) of shear-layer momentum thickness δ_θ and (b) of spreading rate $d\delta_\theta/dz$: Jet0%, Jet3%, Jet6%, Jet9%, Jet12%.

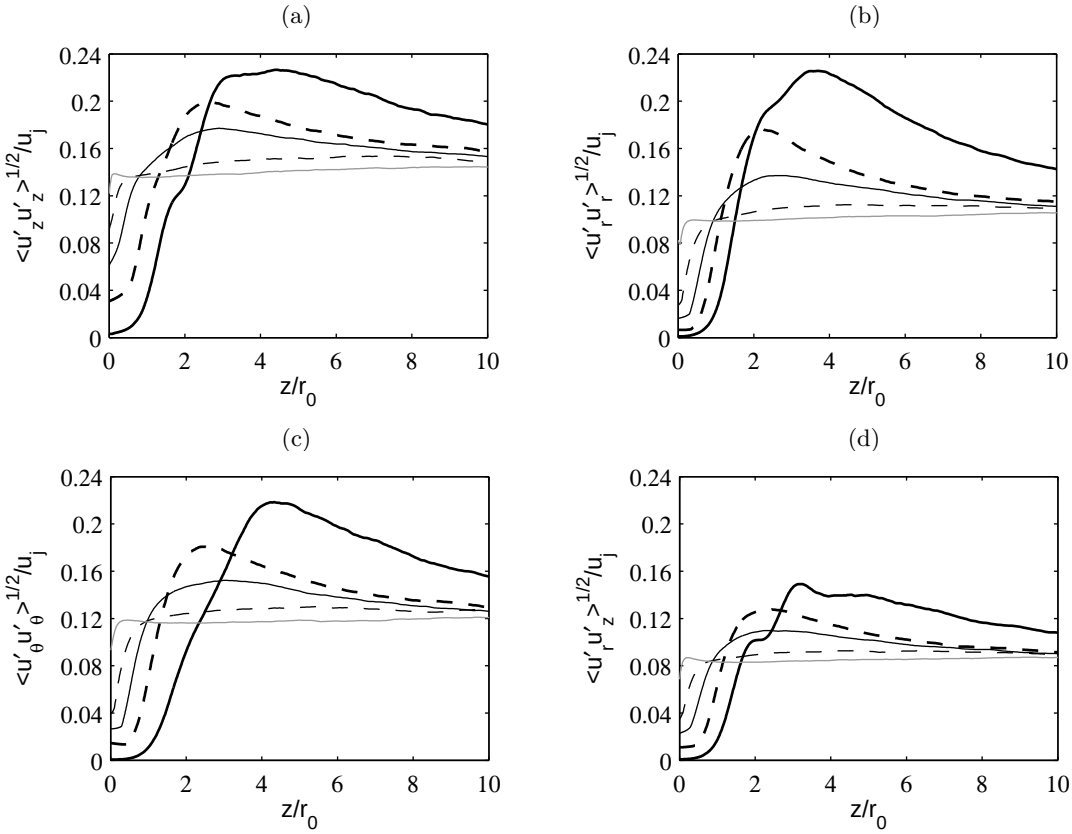

Figure 9. Variations of the peak rms values of fluctuating velocities (a) u'_z, (b) u'_r, (c) u'_θ, and (d) of the peak magnitudes of Reynolds shear stress $<u'_r u'_z>$: Jet0%, Jet3%, Jet6%, Jet9%, Jet12%.

Table 3. Peak rms values of fluctuating velocities u'_z, u'_r and u'_θ in the jets.

	$<u'^2_z>^{1/2}/u_j$	$<u'^2_r>^{1/2}/u_j$	$<u'^2_\theta>^{1/2}/u_j$
Jet0%	22.7%	22.6%	21.8%
Jet3%	19.9%	17.6%	18.1%
Jet6%	17.7%	13.7%	15.2%
Jet9%	15.4%	11.2%	13%
Jet12%	14.5%	10.6%	12.2%

whose maximum rms values with respect to the jet velocity range from 22.6% in Jet0% down to 10.7% in Jet12%, while they are of 17.7% in Jet3%, 13.7% in Jet6% and 11.2% in Jet9%. The turbulence intensity profiles finally increase nearly monotonically in Jet9% and Jet12%, toward values $<u_z'^2>^{1/2}/u_j \simeq 15\%$ and $<u_r'^2>^{1/2}/u_j \simeq 11\%$ for axial and radial velocity components for example. In Jet12%, in particular, the profiles become strikingly flat quickly downstream of the nozzle exit. The present results correspond nicely to those obtained experimentally in axisymmetric mixing layers by Husain and Hussain,[11] also reported in the review paper of Ho and Huerre.[6] The profiles of axial turbulence intensity were indeed found to reach a peak around 19% in the vicinity of the first merging station for laminar initial conditions with $u_e'/u_j \simeq 3\%$, but to relax monotonically to an asymtotic value around 16% for turbulent initial conditions with $u_e'/u_j \simeq 10\%$. Monotonic variations can similarly be noted for the turbulence intensities measured by Arakeri *et al.*[58] in a jet at $\mathrm{Re}_D = 5 \times 10^5$ with $u_e'/u_j \simeq 10\%$, the rms values of axial velocity tending to about 14% of the jet velocity in this case.

Spectra of the fluctuating radial velocity u_r' are finally computed along the lip line at the two axial positions $z = 1.5r_0$ and $z = 3r_0$, and plotted in figures 10(a) and 10(b) respectively, as a function of the Strouhal number St_D. As the turbulence level increases at the jet exit, they become spectacularly broader, but some similarities can be observed. For the initially fully laminar jet in Jet0%, the velocity spectra exhibit pronounced peak frequencies as previously found in Bogey and Bailly.[38] These frequencies correspond approximately to $\mathrm{St}_D = 1.6$ and its sub-harmonics $\mathrm{St}_D = 0.8$, or equivalently to $\mathrm{St}_\theta = f\delta_\theta(0)/u_j = 0.014$ and $\mathrm{St}_\theta = 0.007$ when normalized by the exit boundary-layer thickness. The former St_θ value being typical of frequencies originally predominant in annular mixing layers according to Gutmark and Ho,[5] these results indicate the occurence of roll-ups and pairings of highly coherent vortices in this jet. The velocity spectra in Jet3% and Jet6% display flatter shapes than those in Jet0%, but they are dominated again by components centered around $\mathrm{St}_D \simeq 1.6$ at $z = 1.5r_0$ and $\mathrm{St}_D \simeq 0.8$ at $z = 3r_0$. Weaker but distinguishable vortex pairings therefore take place in the shear layers of these two initially moderately disturbed jets. Based on the velocity spectra, vortex pairings appear even more attenuated in Jet9% and Jet12%, and their presence itself seems questionable. They may however be persistent in Jet9%, as discussed in Bogey *et al.*[39] from acoustic far field properties.

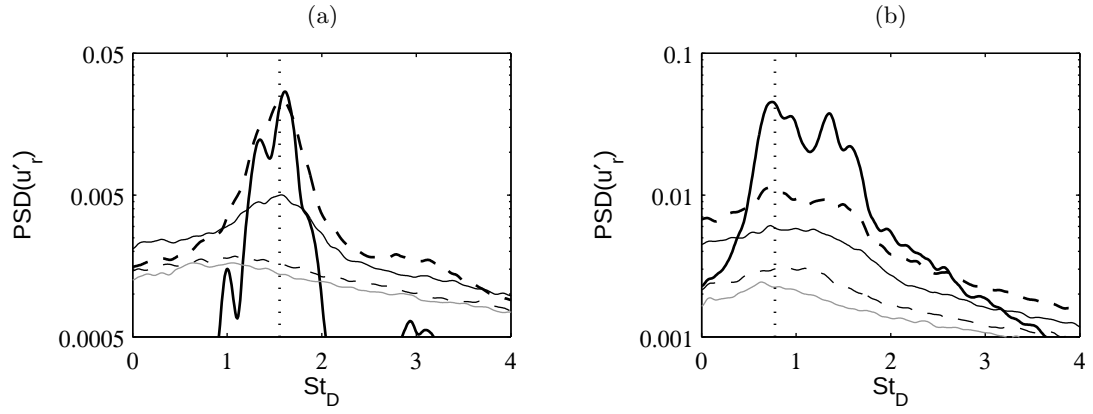

Figure 10. Power spectral densities (PSD) normalized by u_j of radial velocity u_r', (a) at $r = r_0$ and $z = 1.5r_0$ and (b) at $r = r_0$ and $z = 3r_0$, as functions of $\mathrm{St}_D = fD/u_j$: ——— Jet0%, – – – Jet3%, ——— Jet6%, – – – Jet9%, ——— Jet12%. The dotted lines indicates (a) $\mathrm{St}_\theta = f\delta_\theta(0)/u_j = 0.014$ and (b) $\mathrm{St}_\theta = 0.007$.

The present LES results show that the development of the jet shear layers becomes gradually smoother with rising nozzle-exit turbulence intensity. The peak rms values of velocity obtained for turbulent initial conditions, namely for $u_e'/u_j \simeq 10\%$, are in particular roughly half those for fully laminar initial conditions. This is certainely due to the strong weakening, if not the disappearance, of the coherent structures and of their mutual interactions in the former case.

C. Jet flow development

Snapshots of the vorticity norm calculated in the jets up to $z = 25r_0$ are represented in figure 11. With higher turbulence intensities at the nozzle exit, the jets are seen to develop farther downstream, in agreement with the reduction in shear-layer growth rate described in the previous section. Longer potential cores are

visibly obtained. Compare for instance the flow fields in figure 11(a) and in figures 11(d) and 11(e): the end of the potential core is around $z = 10r_0$ in Jet0% but around $z = 15r_0$ in Jet9% and Jet12%.

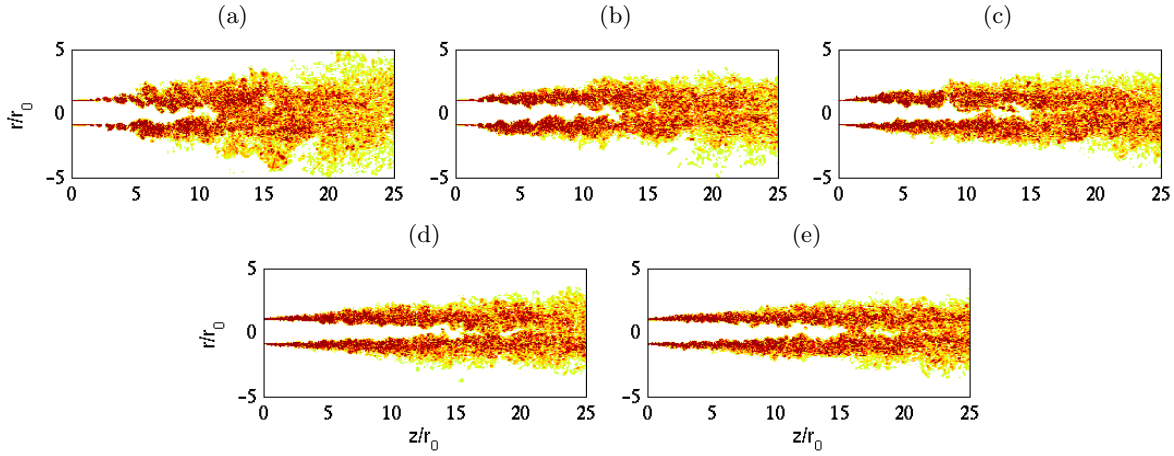

Figure 11. Snapshots in the (z, r) plane of vorticity norm $|\omega|$ in the full jets up to $z = 25r_0$: (a) Jet0%, (b) Jet3%, (c) Jet6%, (d) Jet9%, (e) Jet12%. The colour scale ranges up to the level of $5u_j/r_0$.

The variations of the centerline mean axial velocity u_c and of the jet half-width $\delta_{0.5}$ are shown in figures 12(a) and 12(b). As the turbulence intensity u'_e/u_j rises at the nozzle exit, the velocity decay and the jet spreading both start at increasing axial positions, leading to potential cores ending at $z_c = 9.3r_0$ in Jet0%, $12.9r_0$ in Jet3%, $14.1r_0$ in Jet6%, $15.9r_0$ in Jet9%, and $17r_0$ in Jet12%, where $u_c(z_c) = 0.95u_j$, as reported in table 4. The development of the jet mean flow field is therefore delayed. Downstream of the potential core, it appears more rapid in Jet0% for the untripped, initially fully laminar jet than in the other LESs for the tripped jets. Similar discrepancies between tripped and untripped jets have been found experimentally by Russ and Strykowski,[17] Raman *et al.*[23] and Xu and Antonia,[18] among others. In order to provide more quantitative comparisons, measurements obtained by Lau *et al.*,[57] Arakeri *et al.*[58] and Fleury *et al.*[56] for Mach number 0.9 jets at Reynolds numbers equal to or higher than 5×10^5, thus probably all containing high initial disturbance levels, are also depicted in figure 12. Even if the nozzle-exit conditions in the experimental jets certainly vary, it is interesting to note that these data correspond most favorably to the results from Jet6%.

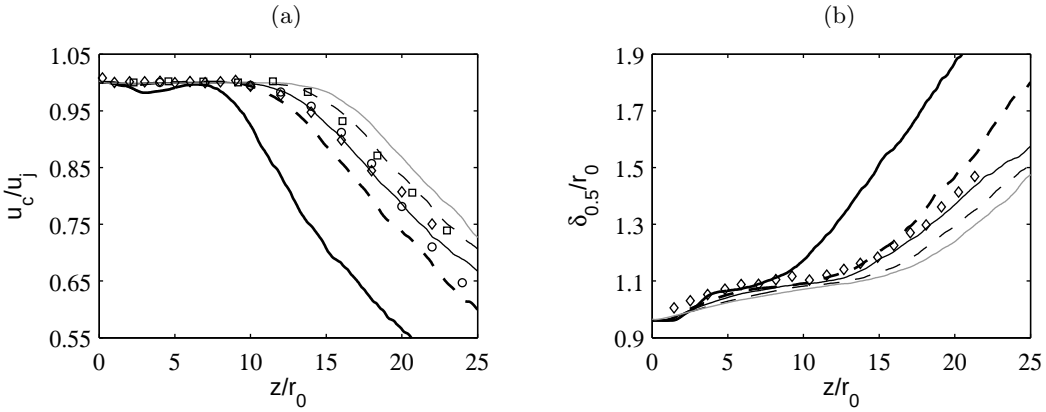

Figure 12. Variations (a) of centerline mean axial velocity u_c and (b) of jet half-width $\delta_{0.5}$: ——— Jet0%, − − − Jet3%, ——— Jet6%, − − − Jet9%, ——— Jet12%. Measurements for Mach 0.9 jets at $Re_D \geq 5 \times 10^5$: ○ Lau *et al.*,[57] □ Arakeri *et al.*,[58] ◇ Fleury *et al.*[56]

The rms values of the axial and radial fluctuating velocities determined along the jet centerline up to $z = 25r_0$ are finally displayed in figures 13(a) and 13(b). For higher nozzle-exit turbulence levels, the peak intensity values are reached farther downstream, in agreement with the delay in mean flow field development. They are reduced for u'_z and u'_r, respectively, from 16.1% and 12.5% in Jet0% down to around 11.5% and 9.3% in Jet9% and Jet12%, refer to table 4 for the peak values in Jet3% and Jet6%. The maximum rms velocities are however rather similar in the four tripped jets, indicating a weak influence of the initial turbulence for

$u'_e/u_j \geq 3\%$. The centerline intensity profiles in this case can also be noticed to compare roughly with the scattered experimental data obtained for Mach number 0.9 jets at Reynolds numbers $\mathrm{Re} \geq 5 \times 10^5$.

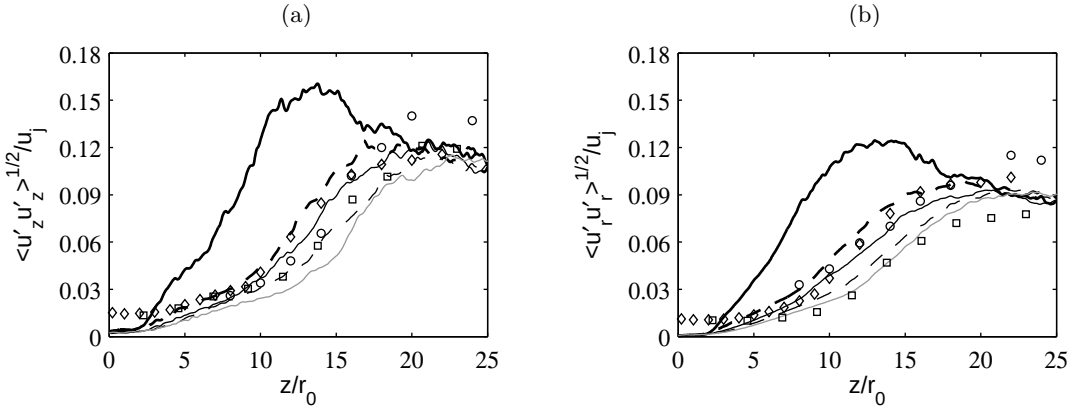

Figure 13. Variations of centerline rms values of fluctuating velocities (a) u'_z and (b) u'_r: ——— Jet0%, – – – Jet3%, ——— Jet6%, – – – Jet9%, ——— Jet12%. Measurements for Mach 0.9 jets at $\mathrm{Re}_D \geq 5 \times 10^5$: □ Arakeri *et al.*,[58] ○ Lau *et al.*,[57] ◇ Fleury *et al.*[56]

Table 4. Axial position of the end of the potential core z_c, and peak rms values of fluctuating velocities u'_z and u'_r on the jet axis.

	z_c/r_0	$<u'^2_z>^{1/2}/u_j$	$<u'^2_r>^{1/2}/u_j$
Jet0%	9.3	16.1%	12.5%
Jet3%	12.9	12.4%	10%
Jet6%	14.1	12.4%	9.3%
Jet9%	15.9	11.4%	9.4%
Jet12%	17	11.5%	9.2%

Except for the monotonic lengthening of the potential core, the impact of the initial turbulence intensity consequently appears relatively limited on the overall jet flow fields. For $u'_e/u_j \geq 3\%$, in particular, the flow field development downstream of the jet core seems to be merely delayed without further notable change.

D. Acoustic fields

In order to provide a first glimpse into the influence of the initial turbulence on the jet acoustic features, snapshots of the fluctuating pressure obtained directly in the LESs are presented in figure 14. The sound fields radiated by the jets are observed to depend significantly on the state of the boundary layers at the nozzle exit, in agreement with the findings of Mollo-Christensen *et al.*,[9] Zaman,[28] Lilley,[24] Bridges and Hussain[29] and Harper-Bourne,[25] to mention a few well-established scientists in the domain. As the exit turbulence intensity increases, the noise levels first appear to decrease dramatically. The peak values of pressure fluctuations are for instance around 300 Pa in figure 14(a) for the initially fully laminar jet, while they are only around 50 Pa in figures 14(d) and 14(e) for the two initially nominally turbulent jets with $u'_e/u_j \simeq 10\%$. The structure of the sound fields is also seen to be modified. Acoustic waves are indeed clearly generated in the shear layers around $z = 5r_0$ in Jet0%, whereas they show a much more complex pattern for the jets with high initial disturbance levels.

The quantitative and qualitative changes in the jet acoustic far fields are examined from the pressure signals obtained at 60 radii from the nozzle exit using the wave extrapolation method documented in section II.D. The sound pressure levels determined at this distance for the different jets are represented in figure 15 for angles ϕ between 30° and 110° relative to the flow direction. They are noticed to decrease considerably with the nozzle-exit peak turbulence intensity for all radiation angles. At $\phi = 90°$, in particular, the noise level is lower by 7.6 dB in Jet3%, 10.1 dB in Jet6%, 12.2 dB in Jet9% and 12.9 dB in Jet12% with respect to the level obtained in Jet0% for the untripped case. Similar observations have been made in experiments on circular jets at moderate Reynolds numbers with laminar or turbulent initial conditions.

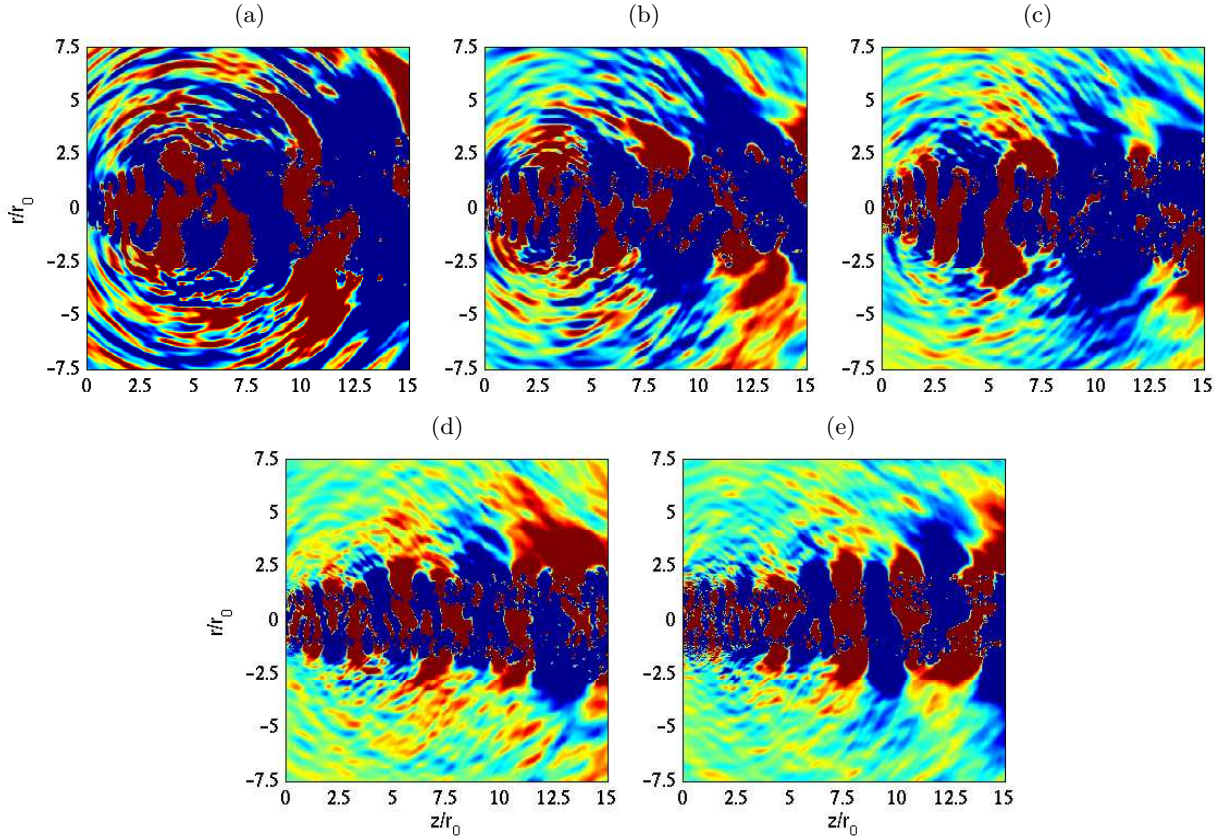

Figure 14. Snapshots in the (z, r) plane of fluctuating pressure $p - p_{amb}$ obtained by LES: (a) Jet0%, (b) Jet3%, (c) Jet6%, (d) Jet9%, (e) Jet12%. The colour scale ranges from -100 to 100 Pa.

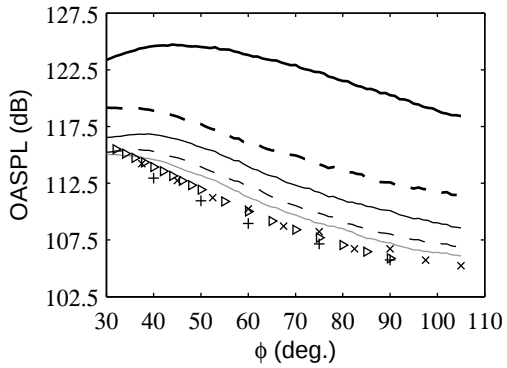

Figure 15. Overall sound pressure levels (OASPL) at $60r_0$ from the pipe exit, as a function of the angle ϕ relative to the jet direction: ——— Jet0%, – – – Jet3%, ——— Jet6%, – – – Jet9%, ——— Jet12%. Measurements for jets at $\mathrm{Re}_D \geq 5 \times 10^5$: + Mollo-Christensen *et al.*,[9] × Lush,[59] ▷ Bogey *et al.*[61]

Zaman[28] for example reported a noise reduction of about 4 dB between an untripped jet and a tripped jet at $\mathrm{Re}_D \simeq 10^5$, in which the exit boundary-layer conditions were $\mathrm{Re}_\theta = 330$ and $u'_e/u_j < 1\%$, and $\mathrm{Re}_\theta = 900$ and $u'_e/u_j \simeq 9\%$, respectively. In the same way, Bridges and Hussain[29] were able to demonstrate that, for two tripped/untripped jets at Reynolds number $\mathrm{Re}_D = 1.4 \times 10^5$, the initially laminar jet with $u'_e/u_j \simeq 0.5\%$ is 2.5 dB louder than the initially turbulent jet. In our previous LESs of Mach number 0.9 round jets, the far-field noise levels at $\phi = 90^o$ were also found to differ by 3 dB in Bogey *et al.*[37] for two jets at $\mathrm{Re}_D = 5 \times 10^5$ with $u'_e/u_j = 1.6\%$ or 9%, and by 8 dB in Bogey and Bailly[38] for two jets at $\mathrm{Re}_D = 10^5$ with $u'_e/u_j = 0.3\%$ or 1.9%.

The sound pressure levels calculated for the different jets are also compared in figure 15 to those measured by Mollo-Christensen *et al.*,[9] Lush[59] and Bogey *et al.*[61] for Mach number 0.9 jets at Reynolds numbers higher than 5×10^5. For all radiation angles, a substantial overestimation is observed for the jet with fully laminar initial conditions, but the agreement becomes much better as the nozzle-exit turbulence intensity increases. At the angle $\phi = 90^o$ for instance, the discrepancy between LES and experimental noise levels is around 4 dB for Jet6%, 2 dB for Jet9% and only 1 dB for Jet12%. Therefore, as the coherent vortices and their interactions are weakened in the jet shear layers, the sound levels clearly tend towards the asymptotically lower levels, in Zaman[20]'s own words, which are reached for initially turbulent jets, and in practice in jets at high Reynolds numbers. The latter jets are indeed very likely to emit negligible vortex pairing noise according to Hussain[4] and Bridges and Hussain.[29] Regarding the possible persistence of vortex noise components of low intensity in Jet9% and Jet12%, suggested by the slightly higher sound levels in these two cases with respect to the measurements, it can be noted that for jets with exit parameters Re_D, Re_θ and u'_e/u_j identical to those in Jet9%, Zaman[28] also obtained a notable deviation compared to the levels extrapolated from high Reynolds number data using classical velocity power laws. As previously mentioned in Bogey *et al.*,[39] this may be due to the combined effects of physical factors such as the flow Reynolds numbers and the initial shear-layer thickness.

The pressure spectra estimated at $60r_0$ from the nozzle exit at the four angles $\phi = 30^o$, 40^o, 60^o and 90^o relative to the jet direction are finally represented in figure 16, together with experimental spectra of Tanna[60] and Bogey *et al.*[61] for Mach number 0.9 jets at $\mathrm{Re}_D \geq 7.8 \times 10^5$. For the initially fully laminar jet in Jet0%, the discrepancies with respect to the measurements are significant for both spectrum level and shape. At the angle $\phi = 30^o$, in figure 16(a), a peak is in particular noticed around $\mathrm{St}_D = 0.8$, which corresponds to the frequency $\mathrm{St}_\theta = 0.007$ of the first vortex pairings in the shear layers as shown in figure 10. At the same radiation angle, the acoustic components around $\mathrm{St}_D \simeq 0.15$ seem also strengthened, as was the case in Bogey and Bailly[38] for two untripped jets at $\mathrm{Re}_D = 10^5$ with $\delta_\theta(0) = 0.023r_0$ and $0.012r_0$. The amplification of the downstream-dominant low-frequency noise component certainly results here from the presence of a thick laminar shear layer, leading to a laminar-turbulent transition occuring in the vicinity of the end of the jet core, and hence to an increase in the rms velocity fluctuations in this region as illustrated in figure 13. With rising initial turbulence levels in the jets, in agreement with the trends exhibited in figure 15, the sound spectra in figure 16 become progressively closer to the high-Re_D experimental spectra at the four radiation angles considered. For Jet9% and in Jet2%, a good agreement with the measurements is thus achieved for Strouhal numbers lower than $\mathrm{St}_D = 0.6$. A slight overestimation by 2-3 dB however persists for $\mathrm{St}_D > 0.6$, which may be attributed to interactions of rather weak laminar-like structures in the present jets at $\mathrm{Re}_D = 10^5$ as discussed above.

IV. Conclusion

In this paper, the influence of the initial turbulence level in jets characterized by identical Mach numbers M and Reynolds numbers Re_D and Re_θ based respectively on the nozzle diameter and the exit boundary-layer momentum thickness is investigated. The effects on the shear-layer features, as well as on the jet development and radiated sound field, are described. They are found to be in good agreement with trends obtained in different experiments, most often dealing either with mixing layers, jet flows or noise, in which several initial flow parameters may vary. In this sense, to the best of our knowledge, the present work is the first one to study the impact, both acoustic and hydrodynamic, of nozzle-exit disturbance intensity on jets under fully controlled conditions.

For the Mach 0.9 jets at $\mathrm{Re}_D = 10^5$ and $\mathrm{Re}_\theta = 10^5$ examined here, the most notable modification in the overall flow development with increasing initial turbulence level is the lengthening of the potential core. For $u'_e/u_j \geq 3\%$ in particular, the flow development downstream of the jet core remains nearly identical. The

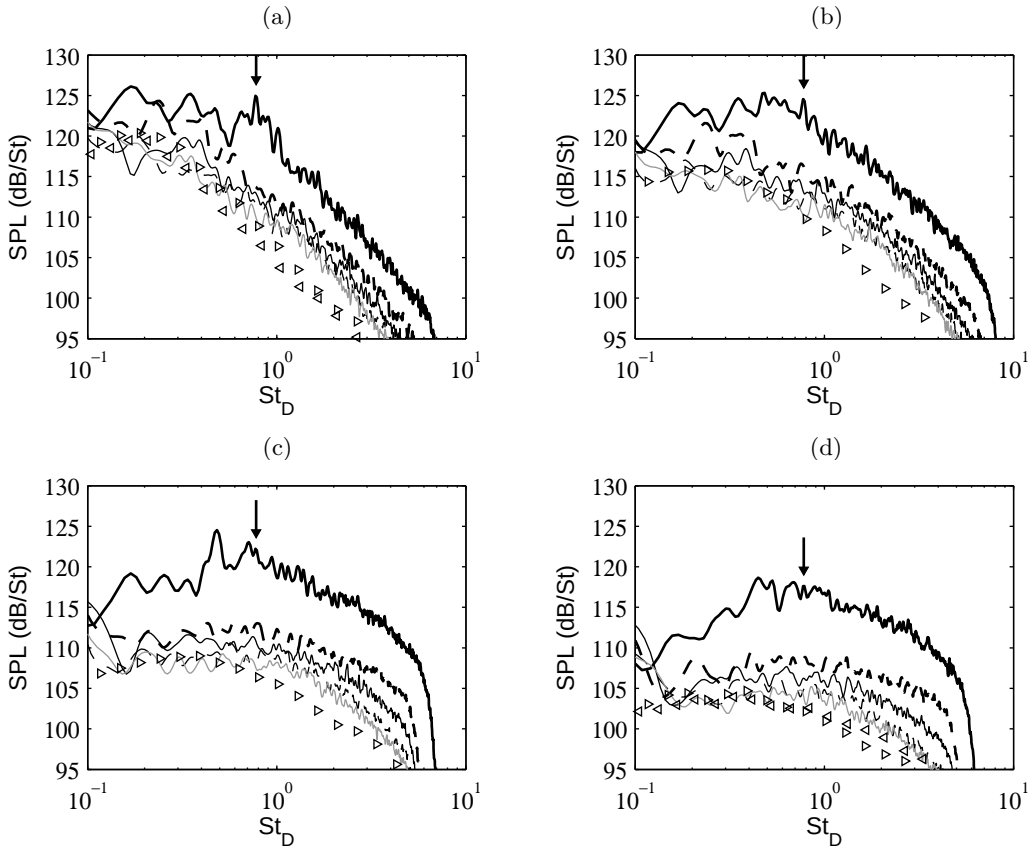

Figure 16. Sound pressure levels (SPL) at $60r_0$ from the jet exit, as a function of $St_D = fD/u_j$, at the angles of (a) $\phi = 30^o$, (b) 40^o, (c) 60^o and (d) 90^o: ——— Jet0%, − − − Jet3%, ——— Jet6%, − − − Jet9%, ——— Jet12%. The arrow indicates the frequency $St_\theta = f\delta_\theta(0)/u_j = 0.007$. Measurements for jets at $Re_D \geq 7.8 \times 10^5$: ◁ Tanna,[60] ▷ Bogey *et al.*[61]

changes are much more spectacular on the shear-layer characteristics and consequently on noise generation. For laminar initial conditions, the mixing layers are clearly dominated by large coherent structures, whose pairings result in a rapid flow development as well as in high turbulence intensities. As the nozzle-exit disturbance intensities increase, these structures become less discernible in the vortical fields, leading to a slower shear-layer spreading and to a strong reduction of the rms velocity peak values, by a factor of about 2 between $u'_e/u_j = 0\%$ and $u'_e/u_j = 10\%$ for instance. Simultaneously, pairing noise components gradually disappear, and the far-field sound levels tend downwards towards those measured for practical jets at high Reynolds numbers. The decrease of the acoustic levels is observed to be significant for low u'_e/u_j, but more limited for higher u'_e/u_j. At the radiation angle of $\phi = 90^o$, for example, they differ by 7.6 dB between Jet0% and Jet3%, 2.5 dB between Jet3% and Jet6%, 1.9 dB between Jet6% and Jet9%, and only 0.7 dB between Jet9% and Jet12%.

These results emphasize the great importance of the initial turbulence in subsonic jet flows. The tendencies found here may however be quantitatively altered if another nozzle-exit boundary-layer thickness (or equivalently another Re_θ) and/or another diameter-based Reynolds number Re_D are considered. The sensitivity of the jet properties to initial turbulence level, and the persistence of vortex pairings in the shear layers may in particular be affected.

Acknowledgments

This work was granted access to the HPC resources of the Institut du Développement et des Ressources en Informatique Scientifique (IDRIS) under the allocation 2011-020204 made by GENCI (Grand Equipement National de Calcul Intensif).

References

[1]Crow, S.C. and Champagne, F.H., "Orderly structure in jet turbulence," *J. Fluid Mech.*, Vol. 48, 1971, pp. 547-591.

[2]Brown, G.L. and Roshko, A., "Density effect and large structure in turbulent mixing layers," *J. Fluid Mech.*, Vol. 64, 1974, pp. 775816.

[3]Crighton, D.G., "Acoustics as a branch of fluid mechanics," *J. Fluid Mech.*, Vol. 106, 1981, pp. 261-298.

[4]Hussain, A.K.M.F., "Coherent structures–reality and myth," *Phys. Fluids*, Vol. 26, No. 10, 1983, pp. 2816-2850.

[5]Gutmark, E. and Ho, C.-M., "Preferred modes and the spreading rates of jets," *Phys. Fluids*, Vol. 26, No. 10, 1983, pp. 2932-2938.

[6]Ho, C.-M. and Huerre, P., "Perturbed free shear layers," *Ann. Rev. Fluid Mech.*, Vol. 23, No. 3, 1984, pp. 365-424.

[7]Hussain, A.K.M.F and Zedan, M.F., "Effects of the initial condition on the axisymmetric free shear layer: Effects of the initial momentum thickness," *Phys. Fluids*, Vol. 21, No. 7, 1978, pp. 1100-1112.

[8]Hussain, A.K.M.F. and Zedan, M.F., "Effects of the initial condition on the axisymmetric free shear layer: Effects of the initial fluctuation level," *Phys. Fluids*, Vol. 21, No. 9, 1978, pp. 1475-1481.

[9]Mollo-Christensen, E., Kolpin, M.A., and Martucelli, J.R., "Experiments on jet flows and jet noise far-field spectra and directivity patterns," *J. Fluid Mech.*, Vol. 18, 1964, pp. 285-301.

[10]Batt, R.G., "Some measurements on the effect of tripping the two-dimensional shear layer," *AIAA J.*, Vol. 13, No. 2, 1975, pp. 245-247.

[11]Husain, Z.D. and Hussain, A.K.M.F., "Axisymmetric mixing layer: influence of the initial and boundary conditions," *AIAA J.*, Vol. 17, No. 1, 1979, pp. 48-55.

[12]Hussain, A.K.M.F. and Husain, Z.D., "Turbulence structure in the axisymmetric free mixing layer," *AIAA J.*, Vol. 18, No. 12, 1980, pp. 1462-1469.

[13]Bell, J.H. and Mehta, R.D., "Development of a two-stream mixing layer from tripped and untripped boundary layers," *AIAA J.*, Vol. 28, No. 12, 1990, pp. 2034-2042.

[14]Chandrsuda, C., Mehta, R.D., Weir, A.D., and Bradshaw, P., "Effect of free stream turbulence on large structure in turbulent mixing layer," *J. Fluid Mech.*, Vol. 85, No. 4, 1978, pp. 693-704.

[15]Wygnanski, I., Oster, D., Fiedler, H., and Dziomba, B., "On the perseverance of a quasi-two-dimensional eddy-structure in a turbulent mixing layer," *J. Fluid Mech.*, Vol. 93, No. 2, 1979, pp. 325-335.

[16]Hill, W.G., Jenkins, R.C., and Gilbert, B.L., "Effects of the initial boundary-layer state on turbulent jet mixing," *AIAA J.*, Vol. 14, No. 11, 1976, pp. 1513-1514.

[17]Russ, S. and Strykowski, P.J., "Turbulent structure and entrainment in heated jets: The effect of initial conditions," *Phys. Fluids A*, Vol. 5, No. 12, 1993, pp. 3216-3225.

[18]Xu, G. and Antonia, R.A., "Effects of different initial conditions on a turbulent free jet," *Exp. Fluids*, Vol. 33, 2002, pp. 677-683.

[19]Zaman, K.B.M.Q. and Hussain, A.K.M.F., "Vortex pairing in a circular jet under controlled excitation. Part 1. General jet response," *J. Fluid Mech.*, Vol. 101, No. 3, 1980, pp. 449-491.

[20]Zaman, K.B.M.Q., "Far-field noise of a subsonic jet under controlled excitation," *J. Fluid Mech.*, Vol. 152, 1985, pp. 83-111.

[21]Lepicovsky, J. and Brown, W.H., "Effects of nozzle exit boundary-layer conditions on excitability of heated free jets," *AIAA J.*, Vol. 27, No. 6, 1989, pp. 712-718.

[22]Raman, G., Zaman, K.B.M.Q., and Rice, E.J., "Initial turbulence effect on jet evolution with and without tonal excitation," *Phys. Fluids A*, Vol. 1, No. 7, 1989, pp. 1240-1248.

[23]Raman, G., Rice, E.J., and Reshotko, E., "Mode spectra of natural disturbances in a circular jet and the effect of acoustic forcing," *Exp. Fluids*, Vol. 17, 1994, pp. 415-426.

[24]Lilley, G.M., "Jet noise classical theory and experiments," in *Aeroacoustics of Flight Vehicles*, Vol. 1, Noise Sources, Ed. H.H. Hubbard, Acoustical Society of America, 1994, pp. 211289.

[25]Harper-Bourne, M., "Jet noise measurements: past and present," *Int. J. of Aeroacoustics*, Vol. 9, No. 4 & 5, 2010, pp. 559-588.

[26]Maestrello, L. and McDaid, E., "Acoustic characteristics of a high-subsonic jet," *AIAA J.*, Vol. 9, No. 6, 1971, pp. 1058-1066.

[27]Grosche, F.-R., "Distributions of sound source intensities in subsonic and supersonic jets," AGARD-CP-131, 1974, pp. 4-1 to 4-10.

[28]Zaman, K.B.M.Q., "Effect of initial condition on subsonic jet noise," *AIAA J.*, Vol. 23, 1985, pp. 1370-1373.

[29]Bridges, J.E. and Hussain, A.K.M.F., "Roles of initial conditions and vortex pairing in jet noise," *J. Sound Vib.*, Vol. 117, No. 2, 1987, pp. 289-311.

[30]Freund, J.B., "Noise sources in a low-Reynolds-number turbulent jet at Mach 0.9," *J. Fluid Mech.*, Vol. 438, 2001, pp. 277-305.

[31]Bogey, C., Bailly, C., and Juvé, D., "Noise investigation of a high subsonic, moderate Reynolds number jet using a compressible LES," *Theoret. Comput. Fluid Dynamics*, Vol. 16, No. 4, 2003, pp. 273-297.

[32]Colonius, T. and Lele, S.K., "Computational aeroacoustics: progress on nonlinear problems of sound generation," *Progress in Aerospace Sciences*, Vol. 40, 2004, pp. 345-416.

[33]Bogey, C. and Bailly, C., "Contributions of CAA to jet noise research and prediction," *Int. J. Comput. Fluid Dyn.*, Vol. 18, No. 6, 2004, pp. 481-491.

[34]Wang, M., Freund J.B., and Lele, S.K., "Computational prediction of flow-generated sound," *Annu. Rev. Fluid. Mech.*, Vol. 38, 2006, pp. 483-512.

[35]Bogey, C. and Bailly, C., "An analysis of the correlations between the turbulent flow and the sound pressure field of subsonic jets," *J. Fluid Mech.*, Vol. 583, 2007, pp. 71-97.

[36]Bogey, C., Barré, S., Juvé, D., and Bailly, C., "Simulation of a hot coaxial jet : direct noise prediction and flow-acoustics correlations," *Phys. Fluids*, Vol. 21, No. 3, 2009, 035105.

[37]Bogey, C., Barré, S., and Bailly, C., "Direct computation of the noise generated by subsonic jets originating from a straight pipe nozzle," *Int. J. of Aeroacoustics*, Vol. 7, No. 1, 2008, pp. 1-22.

[38]Bogey, C. and Bailly, C., "Influence of nozzle-exit boundary-layer conditions on the flow and acoustic fields of initially laminar jets," *J. Fluid Mech.*, Vol. 663, 2010, pp. 507-539

[39]Bogey, C., Marsden, O., and Bailly, C., "Large-Eddy Simulation of the flow and acoustic fields of a Reynolds number 10^5 subsonic jet with tripped exit boundary layers," *Phys. Fluids*, Vol. 23, No. 3, 2011, 035104.

[40]Bogey, C., Marsden, O., and Bailly, C., "On the spectra of nozzle-exit velocity disturbances in initially nominally turbulent jets," submitted to *Phys. Fluids*, 2011.

[41]Bogey, C. and Bailly, C., "A family of low dispersive and low dissipative explicit schemes for flow and noise computations," *J. Comput. Phys.*, Vol. 194, No. 1, 2004, pp. 194-214.

[42]Mohseni, K. and Colonius, T., "Numerical treatment of polar coordinate singularities," *J. Comput. Phys.*, Vol. 157, No. 2, 2000, pp. 787-795.

[43]Bogey, C., de Cacqueray, N., and Bailly, C., "Finite differences for coarse azimuthal discretization and for reduction of effective resolution near origin of cylindrical flow equations," *J. Comput. Phys.*, Vol. 230, No. 4, 2011, pp. 1134-1146.

[44]Bogey, C., de Cacqueray, N., and Bailly, C., "A shock-capturing methodology based on adaptative spatial filtering for high-order non-linear computations," *J. Comput. Phys.*, Vol. 228, No. 5, 2009, pp. 1447-1465.

[45]Berland, J., Bogey, C., Marsden, O., and Bailly, C., "High-order, low dispersive and low dissipative explicit schemes for multi-scale and boundary problems," *J. Comput. Phys.*, Vol. 224, No. 2, 2007, pp. 637-662.

[46]Visbal, M.R. and Rizzetta, D.P., "Large-Eddy Simulation on curvilinear grids using compact differencing and filtering schemes," *J. Fluids Eng.*, Vol. 124, No. 4, 2002, pp. 836-847.

[47]Domaradzki, J.A. and Yee, P.P., "The subgrid-scale estimation model for high Reynolds number turbulence," *Phys. Fluids*, Vol. 12, No.1, 2000, pp. 193-196.

[48]Bogey, C. and Bailly, C., "Large Eddy Simulations of transitional round jets: influence of the Reynolds number on flow development and energy dissipation," *Phys. Fluids*, Vol. 18, No. 6, 2006, 065101.

[49]Bogey, C. and Bailly, C., "Large eddy simulations of round jets using explicit filtering with/without dynamic Smagorinsky model," *Int. J. Heat and Fluid Flow*, Vol. 27, No. 4, 2006, pp. 603-610.

[50]Bogey, C. and Bailly, C., "Turbulence and energy budget in a self-preserving round jet: direct evaluation using large-eddy simulation," *J. Fluid Mech.*, Vol. 627, 2009.

[51]Tam, C.K.W and Dong, Z., "Radiation and outflow boundary conditions for direct computation of acoustic and flow disturbances in a nonuniform mean flow., *J. Comput. Acoust.*, Vol. 4, No. 2,, 1996, pp. 175201.

[52]Ahuja, K.K., Tester, B.J., and Tanna, H.K., "Calculation of far field jet noise spectra from near field measurements with true source location," *J. Sound Vib.*, Vol. 116, No. 3, 1987, pp. 415-426.

[53]Eggels, J.G.M., Unger, F., Weiss, M.H., Westerweel, J., Adrian, R.J., Friedrich, R., and Nieustadt, F.T.M., "Fully developed turbulent pipe flow: a comparison between direct numerical simulation and experiment," *J. Fluid Mech.*, Vol. 268, 1994, pp. 175-209.

[54]Tomkins, C.D. and Adrian, R.J., "Energetic spanwise modes in the logarithmic layer of a turbulent boundary layer," *J. Fluid Mech.*, Vol. 545, 2005, pp. 141-162.

[55]Davies, P.O.A.L., Fisher, M.J., and Barratt, M.J., "The characteristics of the turbulence in the mixing region of a round jet," *J. Fluid Mech.*, Vol. 15, 1963, pp. 337-367.

[56]Fleury, V., Bailly, C., Jondeau, E., Michard, M., and Juvé, D., "Space-time correlations in two subsonic jets using dual-PIV measurements," *AIAA J.*, Vol. 46, No. 10, 2008, pp. 2498-2509.

[57]Lau, J.C., Morris, P.J., and Fisher, M.J., "Measurements in subsonic and supersonic free jets using a laser velocimeter," *J. Fluid Mech.*, Vol. 93, No. 1, 1979, pp. 1-27.

[58]Arakeri, V.H., Krothapalli, A., Siddavaram, V., Alkislar, M.B., and Lourenco, L., "On the use of microjets to suppress turbulence in a Mach 0.9 axisymmetric jet," *J. Fluid Mech.*, Vol. 490, 2003, pp. 75-98.

[59]Lush, P.A., "Measurements of subsonic jet noise and comparison with theory," *J. Fluid Mech.*, Vol. 46, No. 3, 1971, pp. 477-500.

[60]Tanna, H.K., "An experimental study of jet noise. Part I: Turbulent mixing noise," *J. Sound Vib.*, Vol. 50, No. 3, 1977, pp. 405-428.

[61]Bogey, C., Barré, S., Fleury, V., Bailly, C., and Juvé, D., "Experimental study of the spectral properties of near-field and far-field jet noise," *Int. J. of Aeroacoustics*, Vol. 6, No. 2, 2007, pp. 73-92.